Improving skid-steering on a 6x6 all-terrain vehicle: A preliminary experimental study

J.-C. Fauroux[1] LaMI/IFMA/UBP
P. Vaslin[2] LIMOS/UBP
G. Douarre IFMA
Clermont-Ferrand, France

Abstract — *6x6 all-terrain vehicles without a steering system must use great power when skid-steering. In order to increase steering efficiency, it is possible to modify the repartition of normal contact forces on the wheels. This paper describes a preliminary experimental study on the Kokoon vehicle, an all-road 6x6 electric wheelchair. Contact forces of the wheels on the ground are measured via a six component force-plate. Repartition of the normal forces on the six wheels is changed via suspension modification. The first results show that steering can be substantially improved only by minor adjustments on suspension.*

Keywords: all-terrain vehicle (ATV), 6x6, skid-steering, force-plate, Kokoon.

I. Introduction

This paper intends to present preliminary experimental results in order to evaluate the efficiency of skid-steering with a wheeled vehicle. Skid is a phenomenon that appears with every type of ground vehicle when the dynamic forces applied on the vehicle exceed the capabilities of the vehicle-ground interface [1]. Skid may be due to longitudinal inertial forces when accelerating-braking or to lateral inertial forces when steering at high speed and low radius. It may also be due to the design of the vehicle.

Skid always appears with tracked vehicles during turns (even if some of them have front steering tracks [2]) because the long contact surface of the track with the ground cannot be steered without lateral slipping, which induces a reaction torque. On the contrary, wheels ensure a reduced contact surface on a planar ground: a punctual contact with toric tires such as motorbike tires; a linear contact with cylindrical tires, such as those used for cars. In reality, because of tire deformation, the contact point or contact line becomes a contact patch and a moderate steering torque appears. However, wheels have excellent abilities for turning around one diametral axis while keeping ground contact. For tracks as well as wheels, grip depends strongly on the values and distribution of the normal forces [3].

The large majority of wheeled vehicles have steering wheels. It may be the front wheels (in a classical car); the rear wheels (in a power lift truck or lawn mower [4, 5]); all the wheels (on certain types of mobile robots and sport cars [6]); two front and two rear wheels out of six [7] or four front wheels out of eight [8] (on military wheeled armoured vehicles or truck mounted cranes). The steering mechanism is a complex one, particularly when there are more than two steering wheels. Constraints appear such as respecting the Ackermann steering geometry (also known as Jeantaud geometry in Europe) to minimize skid during turns at low speed and being compatible with independent suspension mechanisms. Another drawback of frames with steering wheels is that they generally do not allow to rotate the vehicle on itself without a longitudinal displacement. With two steering wheels, this would mean steering angles around 90°, which is complex to design and dangerous at high speeds.

For this reason, many all-terrain vehicles still rely on fixed wheels with possibly a suspension system but no steering mechanism. Such vehicles have a robust and reliable behaviour on rough terrain. They must turn with skid-steering and behave similarly to tracked vehicles [9]. Most of them have a 4x4 transmission, such as the Pioneer3-AT robot [10], and some have a 6x6 one, such as multi-purpose amphibian vehicles [11]. The purpose of this work is to evaluate the energy consumption of the steering process in a 6x6 configuration and to propose solutions to enhance steering on such types of vehicles with non-directional wheels.

II. Description of the Kokoon vehicle

This paper will use the example of the Kokoon vehicle, an all-road 6x6 electric wheelchair designed by the students of the French Institute for Advanced Mechanics (IFMA) since 1999 [12] (Fig. 1).

The vehicle has two electric motors of 1330W each and is capable to go at 8 km/h on a 20 % slope. Two lead-acid

Fig. 1. Overview of the Kokoon vehicle developed at IFMA since 1999.

[1] E-mail: fauroux@ifma.fr

[2] E-mail: Philippe.Vaslin@isima.fr

batteries ensure a 4h autonomy. Each motor is directly connected to the three wheels on a same side by a transmission mechanism using five belts (Fig. 2 and 3-a). The wheels have independent suspensions with hydro-pneumatic adjustable dampers. The vehicle is 175 cm long and 103 cm wide. The wheelbase is 47 cm and the track width 93 cm. Wheels have a 40 cm diameter. Kokoon was designed to climb easily over 15 cm obstacles.

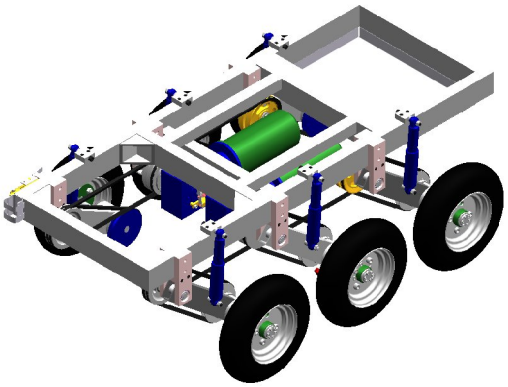

Fig. 2. CAD model of the vehicle frame.

The first tests showed excellent climbing abilities but some difficulties to steer. Even with small tires (tire tread width: 7 cm), the vehicle cannot steer on itself on high adherence grounds such as macadam. Steering is still possible with great turning radii and a non null longitudinal speed.

Initially designed for disabled people, this vehicle is also an interesting research platform because it has a modular design and can be reconfigured easily [13]. This property will allow us to easily modify suspensions (Fig. 3) while keeping unchanged all the other parameters, only by adjusting the location of some critical joints.

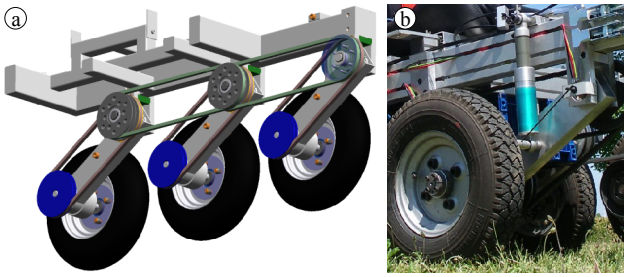

Fig. 3. Belt transmission (a). Adjustable swing arm suspensions (b).

III. Experimental settings

The steering process of a vehicle is a complex phenomenon that may be better understood via an experimental preliminary approach [14, 15]. For this 6x6 vehicle, it was decided to measure experimentally the contact forces of the wheels on the ground.

A. The six-component force-plate

During its displacement, the wheels of the Kokoon vehicle roll on the top plate of a six-component force-plate (TSR, Mérignac, France), rigidly bolted into a wooden box buried in the ground so that the top plate is approximately at the level of the ground (Fig.4 and 5-a).

The six-component force-plate used in this study (Dimensions: 60 x 80 cm - Measurement ranges: F_x = 1000 N, F_y = 900 N, F_z = 2000 N - Resolution: 10 N) is composed of a rigid composite top plate (carbon/aluminium) fixed on three two-component strain gauge force transducers (Fig. 4), which are also firmly fixed on the base plate [16, 17]. Each of these transducers measures one component of the resultant force in the plane of the top plate ("shearing" component: F_x, F_y) and the other in the direction perpendicular to the top plate ("compressive" component: F_z). The signals produced by the six force transducers are multiplied by the thirty-six coefficients of the calibration matrix for calculating the six components (F_x, F_y, F_z, M_x, M_y, M_z) of the wrench applied on the top plate in the reference frame linked to the force-plate (Fig. 5-b). In normal using, the wrench components allow to compute the horizontal coordinates (X, Y) of the point of force application on the force-plate, which is usually called "centre of pressure" (COP).

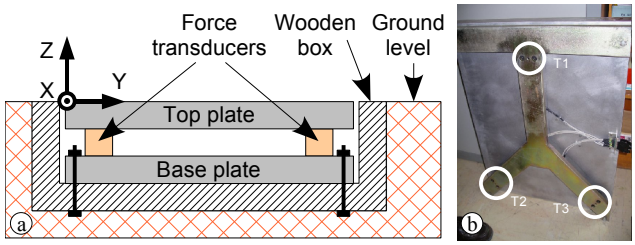

Fig. 4. Setting of the force-plate in the ground (a).
The force-plate including the three transducers (b).

The signals of the force-plate transducers are simultaneously sampled at 100 Hz by a 16-bit A/D conversion card (AT-MIO-16X, National Instruments) slotted into a PC, where experimental data is recorded using an acquisition software (LabView 5.1, National Instruments). The acquisition PC and signal conditioner are brought close to the force platform (Fig. 5-b). Further post-processing is performed in Open Office spreadsheet.

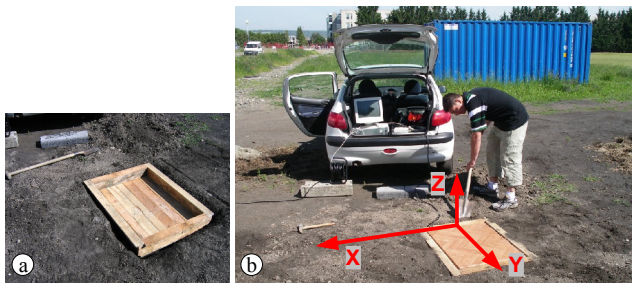

Fig. 5. Integration of the wooden box into the ground (a).
The entire experimental system (b).

B. Centre of mass

Mass repartition on the wheels has a great influence on the ground contact. It is determined independently by three

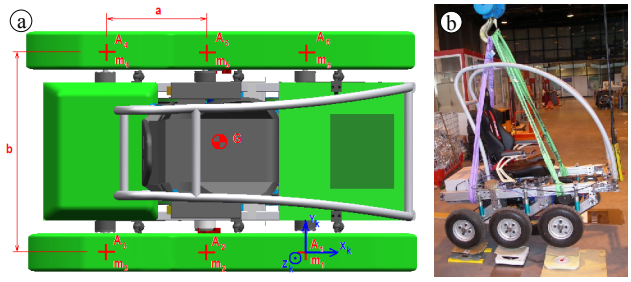

Fig. 6. Computing the centre of mass on the CAD model (a). Measuring the weight repartition with six scales (b).

different methods and results are coherent.

The first method uses the CAD model of Kokoon (Fig. 6-a). Each component is given a uniform density (approximate assumption) and the Solid Edge CAD software can evaluate the volume and calculate the weight of the component. The whole assembly, including several hundreds of parts, reaches a total weight of about 367 kg without external composite panels.

The second method consists in putting delicately the vehicle on six scales with a winch (Fig. 6-b). The results are summarized in Table I and are very close to those obtained with the first method. The longitudinal position X_G of the centre of mass G is also given relatively to the middle axle. G is located 133 mm behind the middle axle without driver and only 78 mm behind with a 83 kg driver, for a total weight of 450 kg. The load is higher on the rear axle and secondly on the middle axle, even if the driver mass contributes to re-centre point G.

The third method relies on the force-plate to measure static loads on each wheel. The results are also perfectly coherent and will be commented later (Fig. 10-a).

	Front axle (kg)	Middle axle (kg)	Rear axle (kg)	Total (kg)	X_G (mm)
Without driver	66	129	171	367	-133
With a 83kg driver	108	158	183	450	-78

TABLE I. Mass repartition on the axles and position of the centre of mass.

C. Modifying the suspensions

This paper focuses on improving steering efficiency of multi-axle vehicles such as Kokoon. One solution may be to modify mass repartition. This can be done by physically adding mass or moving existing components and payload in the frame.

Another simpler solution is to modify suspension characteristics. In this work, we choose to modify the central suspension relatively to the front and rear suspensions. Our purpose is to increase the vertical load on the central axle, which is equivalent to unload the front and rear axles.

The suspension mechanism is represented in Fig. 7 with its main dimensions. For simplicity reasons, it was chosen to change the h_s length from $h_{s\,std}$ = 145 mm to the minimal possible length $h_{s\,mod}$ = 45 mm. This was obtained by translating forward the top-attachment points of the front and rear dampers in their T-slot.

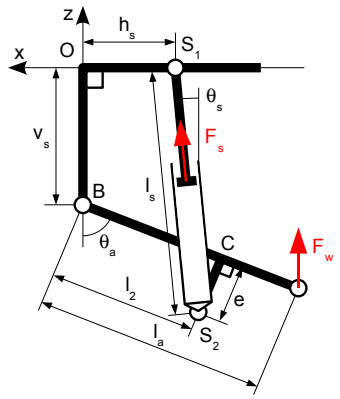

Parameter	Value
v_s	180 mm
$h_{s\,std}$	145 mm
$h_{s\,mod}$	45 mm
l_s	210-280 mm
l_2	170 mm
l_a	350 mm
e	15 mm

Fig. 7. The suspension mechanism with its dimensions.

By changing h_s of 100 mm, the stiffness of the middle suspension is reinforced and the initial vertical position of the central wheel is changed. Most of all, the central axle is strongly overloaded, which is visible on Fig. 8-b.

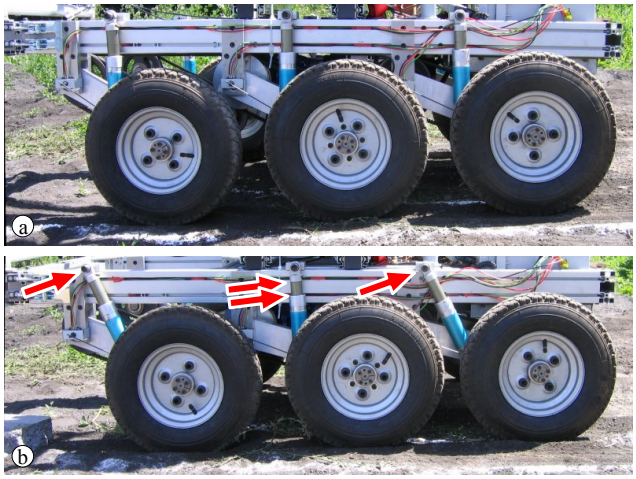

Fig. 8. Standard suspension configuration (a). Modified configuration (b).

Table II summarizes the changes in weight repartition. Front and rear axles are off-loaded of 26% and 35% respectively while middle axle bears 58% more.

	Front axle (kg)	Middle axle (kg)	Rear axle (kg)	Total (kg)
Standard configuration	108	158	183	450
Modified configuration	80 (-26%)	250 (+58%)	120 (-35%)	450

TABLE II. Changing mass repartition (including a 83kg driver).

IV. Experimental results

A. Reference 6x6 vehicle with standard suspension

The experimental setting can be seen on Fig. 9. Lines showing the desired trajectories are drawn on the ground with flour. Three types of trajectories are considered in this work: a straight line (which is equivalent to a turn with infinite radius); a turn with 6m radius; a turn with 3 m radius. Several experiments were performed in the aim of following as much as possible the desired trajectories. Results are summarized in Fig. 10.

The acquisition frequency is 1/100th of second, which is enough for a low speed vehicle such as Kokoon. Test duration varies according to the the trajectory: rolling straight forward takes generally no more than 1.5 s (Fig. 10-a) while turning is slower and requires around 2.5 s (Fig 10-b-c) because steering requires much power from the electric motors and this power must be adjusted in real time by the driver on each side of the vehicle.

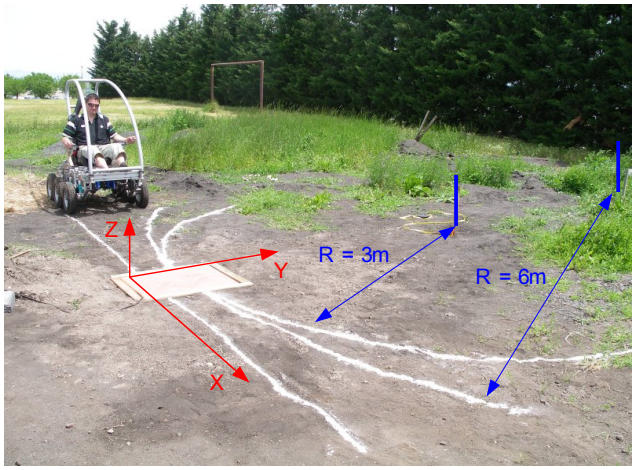

Fig. 9. Experimental setting with reference frame and trajectories.

Fig. 10-a shows the reaction forces applied to the vehicle when rolling straight forward. Because the base wheel of the vehicle (47 cm) is smaller than the force-plate width along the rolling direction (60 cm), it occurs that there are sometimes one and sometimes two wheels at the same time on the force-plate. This explains the shape of the curves. The time axis can be divided into five phases:

1. First, only wheel 1 applies efforts on the platform;
2. Then wheel 2 climbs on the platform (left transparent area) and the vertical component of reaction force R_z increases suddenly;
3. After that, wheel 1 goes out of the platform and only wheel 2 remains on it;
4. Then, it is up to wheel 3 to go on the platform (right transparent area) and another peak on R_z appears;
5. Finally, wheel 2 leaves the platform and only wheel 3 remains on it.

Table III is obtained by averaging the R_x, R_y, R_z values on the single wheel intervals and gives an order of magnitude of the reaction components, thus eliminating the small variations in the signal due to electrical perturbations and vehicle vibrations on small gravels.

Concerning normal force R_z, it can be seen that wheel 3 (930 N) bears more than wheel 2 (848 N) which bears more than wheel 1 (635 N). These results include the driver weight and confirm the previous calculations of the centre of mass. If grip coefficient is supposed equivalent on each wheel, this means that the rear and central wheels are able to apply a higher propulsion force R_x and to undergo a higher lateral force R_y. When the trajectory varies (Fig. 10-b and 10-c), the overall shape of the R_z normal force does not change a lot: the first peak is identical; the second peak changes a little, probably because of transient phenomena.

The propulsion force R_x has an original shape: it seems that only the central wheel applies a propulsion force. This could be probably justified by insufficient tension in the front and rear transmission belts. It should be corrected very soon because the central belts cannot transmit the complete torque so only one third of the potential propulsion force is currently used by the vehicle. Another interesting point is about the evolution of R_x with the steering radius R: when R decreases, R_x must increase to make the vehicle rotate. Along a straight line, R_x does not need to be very high to generate vehicle movement. But during a turn with R = 6 m (respectively 3 m), R_x reaches 454 N (resp. 553 N). This is clearly felt by the driver, who needs to increase the power for small turns.

The lateral force R_y has a negligible value when rolling straight forward. This value increases particularly on front and rear wheels when the turning radius R decreases. For instance, for the 3 m turn, R_x has a value of -321 N (resp. 532 N) on wheel 1 (resp. wheel 3). The signs are opposite, which is normal. The absolute values of R_y are not symmetrical, probably because they are proportional to R_z. Another possible explanation would be that the instant rotation centre of the vehicle is not exactly on the the central axle axis (trajectory error). This is probably the case for the 3 m turn, where R_y is non null on the central wheel (-146 N).

B. Modified 6x6 vehicle

On the modified vehicle, test duration during turn takes only 2 s (Fig. 11-b-c) instead of 2.5 s (Fig. 10-b-c) because steering and power control are much easier for the vehicle and the driver respectively. These improvements were clearly experienced by the driver during tests.

For the straight line trajectory (Fig. 11-a), the normal force R_z has a strange shape with a peak during Phase 3. This might be caused by forward leaning of the driver or by vehicle tilting on a small obstacle. On Fig. 11-a-b-c, it can be noticed that the R_z curve does not change a lot with the turning radius R.

For propulsion force R_x, the curves still show that only the central wheel applies a propulsion force. However, the modified suspension seems to have decreased the propulsion force. This means that a smaller force generates the same movement. For a 6 m turn, R_x decreases from 454 N to 282 N, which means a 38% gain. The driver needs to inject fewer energy in the electric motors. Moreover, as the overall turning time is shorter than with classical suspension, it can be concluded that the global turning efficiency is definitely improved.

The lateral force R_y has more or less the same shape in Fig. 11 as in Fig. 10. For a 6 m turn whith the modified vehicle, there is a 28% decrease of R_y on the front axle and a 36% decrease on the rear axle. This means fewer energy dissipated during skid-steering.

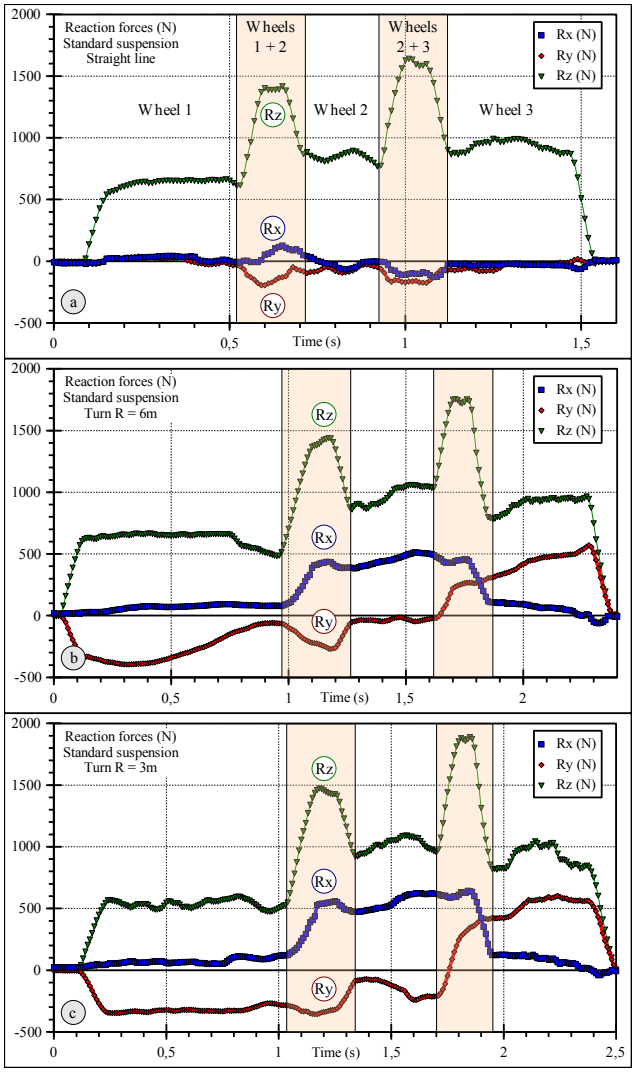

Fig. 10. Forces on the right wheels for the standard suspension.

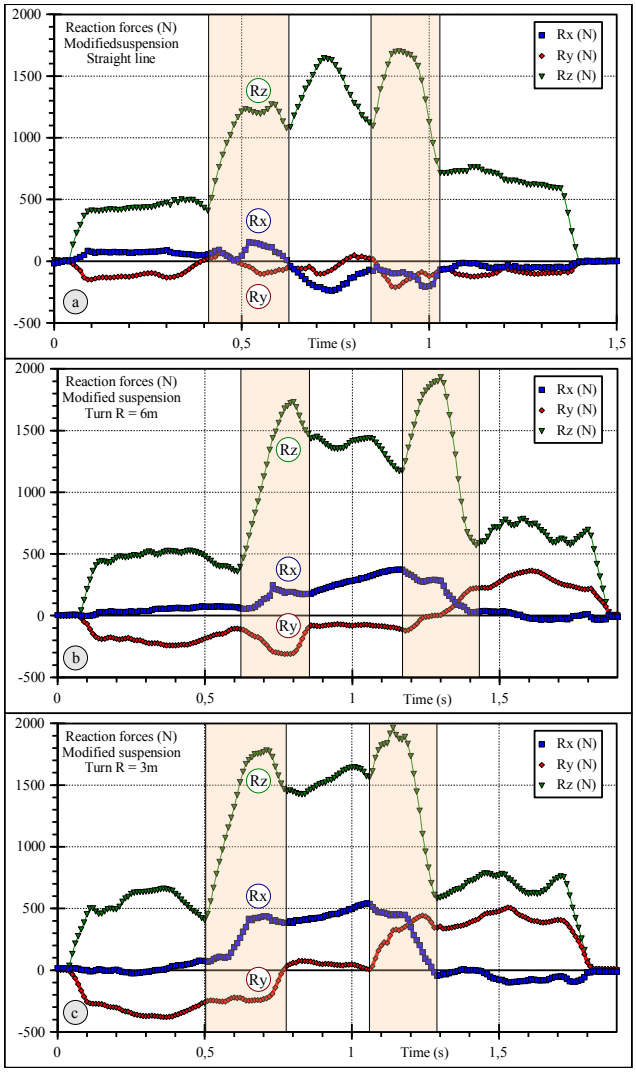

Fig. 11. Forces on the right wheels for the modified suspension.

Standard suspensions	Wheel 1 (Front)			Wheel 2 (Middle)			Wheel 3 (Rear)		
	R_X (N)	R_Y (N)	R_Z (N)	R_X (N)	R_Y (N)	R_Z (N)	R_X (N)	R_Y (N)	R_Z (N)
Straight line	23	10	635	-17	-67	848	-30	-40	930
Turn R = 6m	70	-270	627	454	-36	972	68	438	905
Turn R = 3m	74	-321	534	553	-146	1016	86	532	914

TABLE III. Average forces on the right wheels for standard suspensions.

Modified suspensions	Wheel 1 (Front)			Wheel 2 (Middle)			Wheel 3 (Rear)		
	R_X (N)	R_Y (N)	R_Z (N)	R_X (N)	R_Y (N)	R_Z (N)	R_X (N)	R_Y (N)	R_Z (N)
Straight line	69	-105	446	-155	-33	1393	-43	-95	671
Turn R = 6m	49	-194	468	282	-80	1382	3	281	671
Turn R = 3m	8	-331	563	450	49	1533	-55	398	666

TABLE IV. Average forces on the right wheels for modified suspensions.

Another experimental result is represented in Fig. 12: the trace of the centre of pressure on the force-plate for different trajectories of the modified vehicle. Phases 1, 3 and 5 are represented by a curve segment going upward. Phases 2 and 4 (where two wheels are present at the same time on the platform) are represented by a sudden inflexion of the curve downward. It is interesting to see that the centre of pressure follows quasi-perfect arcs of circles during phases 1-3-5. This confirms that trajectory was correctly followed (see arrows on Fig. 12).

C. Some elements of physical explanation

These preliminary results are quite encouraging and tend to suggest that turning efficiency is highly sensitive to mass repartition. This phenomenon can be partially explained by existing results. In [18], Halconruy shows that the lateral force R_y is a function of the slip angle α_s. The beginning of the curve is linear (Fig. 13-a) up to a limit angle α_{sl}, which is of the order of 10° for a typical car tire. Above this threshold, there is a transition zone and the tire starts to slip on the ground. It has also been proved that the lateral force R_y depends on the normal force R_z. An increment on R_z generates an increment on R_y. This phenomenon is exactly what was noticed during our experiments.

The slip angle α_s is the angle between the median plane of the tire and rolling direction. There is a direct relation between α_s, trajectory and vehicle geometry.

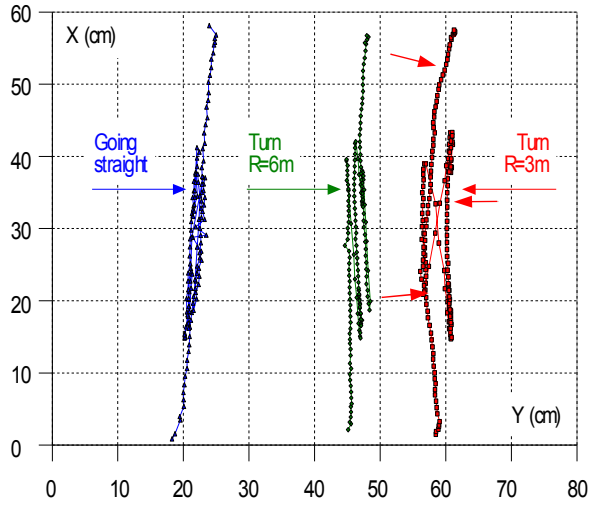

Fig. 12. Trace of the centre of pressure for the modified vehicle and for three types of trajectories.

If the centre of rotation of the vehicle is supposed to be located on the middle axle, slip angles α_{s1} and α_{s2} appear on the front and rear axles of the skid-steering vehicle (Fig. 13-b). Larger wheelbase and smaller turning radius generate higher slip angles. Consequently, lateral forces increase and the vehicle needs more energy to turn.

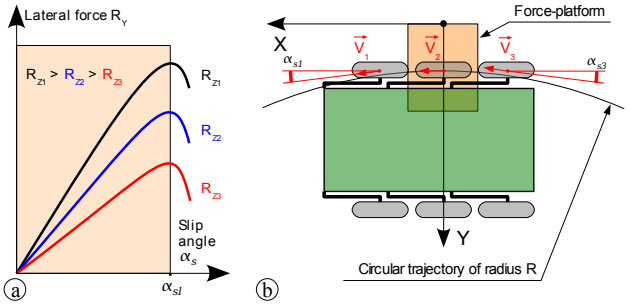

Fig. 13. The lateral force depends on slip angle and normal force (a). The slip angles depend on trajectory and vehicle geometry (b).

VI. Conclusion

This preliminary experimental work proved that steering efficiency of the 6x6 all-terrain Kokoon vehicle can be substantially improved only by minor adjustments on the vehicle suspension. An important modification in weight repartition was obtained by a 10 cm adjustment on damper fixtures. This minor adjustment allowed to reduce the propulsion forces of about 20-30 % and also decreased the lateral forces in the same proportion. The driver also reported that he felt a substantial improvement of steering capacities during tests with the modified vehicle.

This method could be generalized to many types of multi-axle vehicles in order to improve their steering performance. The absence of any steering system on a vehicle is a guarantee of robustness and control simplicity but has the drawback of high power consumption during steering phases. With such a solution, one can imagine an adaptative suspension capable of modifying normal force repartition on the wheels without changing neither mass nor payload repartition in the vehicle. This is currently done manually. In a future version, the suspension adjustment could be performed automatically during turns by a dedicated mechanism.

Further work will focus on extended experimental results including measurements on all the wheels of the vehicle and an analytical model of the involved phenomena.

Acknowledgement

The Kokoon prototype was designed with financial support of ANVAR (French National Agency for Development of Research) and MICHELIN company. The other sponsors and people involved in Kokoon development are given on the Kokoon Project web page: http://www.kokoon.fr.st

References

[1] Kececi E.F., and Tao G. Adaptive vehicle skid control. *Mechatronics*, 16(5):291-301, June 2006.
[2] Watanabe K., Kitano M., and Fugishima A. Handling and stability performance of four-track steering vehicles. *Journal of Terramechanics*, 32(6):285-302, November 1995.
[3] Mokhiamar O., and Abe M. How the four wheels should share forces in an optimum cooperative chassis control. *Control Engineering Practice*, 14(3):295-304, March 2006.
[4] Besselink B. C. Development of a vehicle to study the tractive performance of integrated steering-drive systems. *Journal of Terramechanics*, 41(4):187-198, October 2004.
[5] Besselink B. C. Computer controlled steering system for vehicles having two independently driven wheels. *Computers and Electronics in Agriculture*, 39(3):209-226, August 2003.
[6] Shoichi S., Yoshimi F. and Yutaka T. *Steering apparatus for a vehicle having steerable front and rear wheels*. Patent number US4614351, 1986-09-30, Honda Motor Co Ltd (Japan).
[7] FNSS Corp., PARS 6x6 and 8x8 Wheeled Armoured Vehicles, http://www.fnss.com.tr
[8] Patria Corp., The Armoured Modular Vehicle, http://www.patria.fi.
[9] Maclaurin B. A skid steering model with track pad flexibility. *Journal of Terramechanics*, In Press, Corrected Proof, Available online 9 June 2006.
[10] Robosoft Corp. The Pioneer 3 ATRV. http://www.robosoft.fr.
[11] Oasis LLC Corp. The Max 6x6 ATV. http://www.oasisllc.com/english/max.htm
[12] Fauroux J.C., Charlat S., and Limenitakis M. Team design process for a 6x6 all-road wheelchair. In *Proc. International Engineering and Product Design Education Conference,* pp. 315-322, *IEPDE'2004*, Delft, The Netherlands, September 2nd - 3rd, 2004.
[13] Fauroux J.C., Charlat S., and Limenitakis M. Conception d'un véhicule tout-terrain 6x6 pour les personnes à mobilité réduite. In *Proc. 3ème conférence Handicap 2004*, June 17th - 18th, 2004, Paris Expo, Porte de Versailles / France, pp. 59-64.
[14] Itoh H. , Oida A. and Yamazaki M. Measurement of forces acting on 4WD-4WS tractor tires during steady-state circular turning in a rice field. *Journal of Terramechanics*, 32(5):263-283, September 1995.
[15] Foster J.R., Ayers P.D., Lombardi-Przybylowicz A.M. and Simmons K. Initial effects of light armored vehicle use on grassland vegetation at Fort Lewis, Washington. *Journal of Environmental Management*, In Press, Corrected Proof, Available online 23 March 2006.
[16] Couétard Y. *Capteur de forces à deux voies et application notamment à la mesure d'un torseur de forces*. INPI, Brevet N° 96 08370 (France), 1993.
[17] Couétard Y. *Caractérisation et étalonnage de dynamomètres à six composantes pour torseur associé à un système de forces.* PHD thesis report, Bordeaux 1 University, 2000.
[18] Halconruy T. *Les liaisons au sol. 1995, 200p.,* E.T.A.I.